

# Phenomenology of Higgsless Models at the LHC and the ILC

Andreas Birkedal\*, Konstantin T. Matchev

*Institute for Fundamental Theory, University of Florida, Gainesville, FL 32611, USA*

Maxim Perelstein

*Institute for High-Energy Phenomenology, Cornell University, Ithaca, NY 14853, USA*

We investigate the signatures of the recently proposed Higgsless models at future colliders. We focus on tests of the mechanism of partial unitarity restoration in the longitudinal vector boson scattering, which do not depend on any Higgsless model-building details. We study the LHC discovery reach for charged massive vector boson resonances and show that all of the preferred parameter space will be probed with  $100 \text{ fb}^{-1}$  of LHC data. We also discuss the prospects for experimental verification of the Higgsless nature of the model at the LHC. In addition, in this talk we present new results relevant for the discovery potential of Higgsless models at the International Linear Collider (ILC).

## 1. INTRODUCTION

One of the greatest unsolved mysteries of the Terascale is the origin of electroweak symmetry breaking (EWSB). Within the usual description of the Standard Model (SM), a weakly coupled Higgs boson performs this task. However, it has still not been experimentally verified whether electroweak symmetry is broken by such a Higgs mechanism, by strong dynamics [1], or by something else. This is one of the crucial questions particle physicists hope to answer in the upcoming experiments at the Large Hadron Collider (LHC) at CERN.

Experiments have already been able to put some constraints on theoretical ideas about EWSB. In theories involving EWSB by strong dynamics, the scale  $\Lambda$  at which new physics enters can be guessed from the scale at which massive gauge boson scattering becomes non-unitary. A simple estimate gives a value of

$$\Lambda \sim 4\pi M_W/g \sim 1.8 \text{ TeV}, \quad (1)$$

which is disfavored by precision electroweak constraints (PEC) [2]. Thus, strong dynamics would seem to be largely ruled out as the source of EWSB. However, a new class of models, termed “Higgsless” [3–6], have been able to raise the scale of strong dynamics, allowing agreement with PEC [7].

Realistic Higgsless models contain new TeV-scale weakly coupled states accessible at the LHC. Among those, there are new massive vector bosons (MVB), heavy cousins of the  $W$ ,  $Z$  and  $\gamma$  of the SM, which are of primary interest. It is those states that delay unitarity violation and hence allow the scale  $\Lambda$  to be raised [8]. Unfortunately, the details of the fermion sector of the theory are highly model-dependent. For instance, initial Higgsless models did not allow sufficient change in  $\Lambda$  to agree with PEC [9–11], and modifications of the fermion sector were necessary. However, the basic mechanism by which  $\Lambda$  is raised is identical in all “Higgsless” models, even regardless of the number of underlying dimensions [12]. It is this mechanism that was studied in [13], focusing on its collider signatures. In this talk, we will review the analysis of Ref. [13], and present some new results, relevant for the International Linear Collider (ILC). In Sec. 2 we derive a set of sum rules which should be obeyed by the couplings between the new MVBs and the SM  $W/Z$  gauge bosons. We identify discovery signatures of the new MVBs at the LHC which only rely on the couplings guaranteed by the sum rules, and compare to the SM Higgs search signals. In Sec. 3 we discuss the LHC reach for charged MVBs and methods for testing the sum rules of Sec. 2 in order to identify the “Higgsless” origin of the MVB resonances. In Sec. 4 we discuss the corresponding Higgsless phenomenology at the ILC.

---

\*This talk was given by A. Birkedal, describing past and ongoing work performed in collaboration with the other authors.

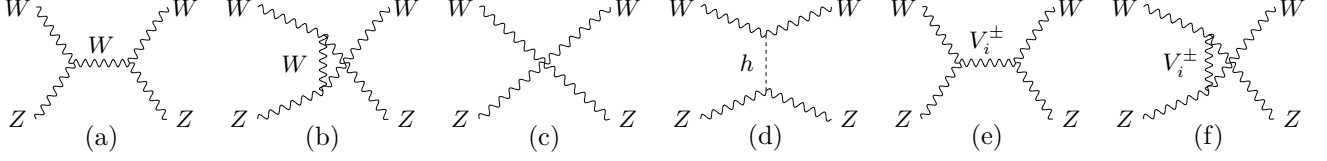


Figure 1: Diagrams contributing to the  $W^\pm Z \rightarrow W^\pm Z$  scattering process: (a), (b) and (c) appear both in the SM and in Higgsless models, (d) only appears in the SM, while (e) and (f) only appear in Higgsless models.

## 2. UNITARITY SUM RULES

Consider the elastic scattering process  $W_L^\pm Z_L \rightarrow W_L^\pm Z_L$ . In the absence of the Higgs boson, this process receives contributions from the three Feynman diagrams shown in Figs. 1(a)–(c). The resulting amplitude contains terms which grow with the energy  $E$  of the incoming particle as  $E^4$  and  $E^2$  and ultimately cause violation of unitarity at sufficiently high energies. In the SM, both of these terms are precisely cancelled by the contribution of the Higgs exchange diagram in Fig. 1(d). In the Higgsless theories, on the other hand, the diagram of Fig. 1(d) is absent, and the process instead receives additional contributions from the diagrams in Figs. 1(e) and 1(f), where  $V_i^\pm$  denotes the charged MVB of mass  $M_i^\pm$ . The index  $i$  corresponds to the KK level of the state in the case of a 5D theory, or labels the mass eigenstates in the case of a 4D deconstructed theory. Remarkably, the  $E^4$  and  $E^2$  terms can again be exactly cancelled by the contribution of the MVBs, provided that the following sum rules are satisfied [13]:

$$g_{\text{wwzz}} = g_{\text{wwz}}^2 + \sum_i (g_{\text{wzv}}^{(i)})^2, \quad (1)$$

$$2(g_{\text{wwzz}} - g_{\text{wwz}}^2)(M_W^2 + M_Z^2) + g_{\text{wwz}}^2 \frac{M_Z^4}{M_W^2} = \sum_i (g_{\text{wzv}}^{(i)})^2 \left[ 3(M_i^\pm)^2 - \frac{(M_Z^2 - M_W^2)^2}{(M_i^\pm)^2} \right]. \quad (2)$$

Here  $M_W$  ( $M_Z$ ) is the  $W$ -boson ( $Z$ -boson) mass and the notation for the triple and quartic gauge boson couplings is self-explanatory. In 5D theories, these equations are satisfied exactly if all the KK states,  $i = 1 \dots \infty$ , are taken into account. This is not an accident, but a consequence of the gauge symmetry and locality of the underlying theory. While this is not sufficient to ensure unitarity at all energies (the increasing number of inelastic channels ultimately results in unitarity violation), the strong coupling scale can be significantly higher than the naive estimate (1). For example, in the warped-space Higgsless models [4, 7] unitarity is violated at the scale [14]

$$\Lambda_{\text{NDA}} \sim \frac{3\pi^4 M_W^2}{g^2 M_1^\pm}, \quad (3)$$

which is typically of order 5–10 TeV. In 4D models, the number of MVBs is finite and the second of the sum rules (2) is only satisfied approximately; however, our numerical study of sample models indicates that the violation of the sum rule has to be very small (at the level of 1%) to achieve an adequate improvement in  $\Lambda$ .

Considering the  $W_L^+ W_L^- \rightarrow W_L^+ W_L^-$  scattering process yields sum rules constraining the couplings of the neutral MVBs  $V_i^0$  (with masses denoted by  $M_i^0$ ) [3]:

$$g_{\text{wwww}} = g_{\text{wwz}}^2 + g_{\text{ww}\gamma}^2 + \sum_i (g_{\text{wwv}}^{(i)})^2, \quad (4)$$

$$4g_{\text{wwww}} M_W^2 = 3 \left[ g_{\text{wwz}}^2 M_Z^2 + \sum_i (g_{\text{wwv}}^{(i)})^2 (M_i^0)^2 \right].$$

Considering other channels such as  $W_L^+ W_L^- \rightarrow ZZ$  (see Fig. 2) and  $ZZ \rightarrow ZZ$  does not yield any new sum rules. The presence of multiple MVBs, whose couplings obey Eqs. (2), (4), is a generic prediction of the Higgsless models.

Our study of the collider phenomenology in the Higgsless models will focus on the vector boson fusion processes. These processes are attractive for two reasons. Firstly, the production of MVBs via vector boson fusion is relatively

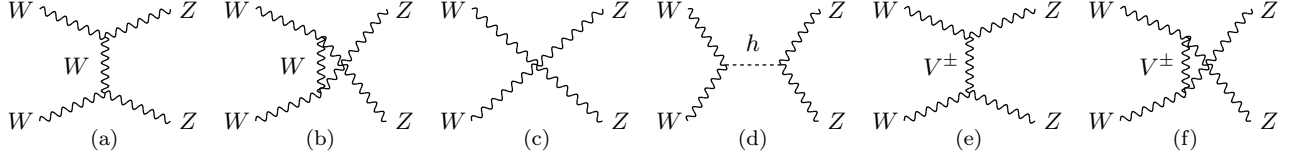


Figure 2: Diagrams contributing to the  $W^\pm W^\mp \rightarrow ZZ$  scattering process: (a), (b) and (c) appear both in the SM and in Higgsless models, (d) only appears in the SM, and (e) and (f) only appear in Higgsless models.

model-independent, since the couplings are constrained by the sum rules (2), (4). This is in sharp contrast with the Drell-Yan production mechanism [10], which dominates for the conventional  $W'$  and  $Z'$  bosons but is likely to be suppressed for the Higgsless MVBs due to their small couplings to fermions, as needed to evade PEC [7]. In the following, unless specified otherwise, we shall assume that the MVBs have no appreciable couplings to SM fermions. Secondly, if enough couplings and masses can be measured, these processes can provide a *test* of the sum rules, probing the mechanism of partial unitarity restoration.

Eq. (3) indicates that the first MVB should appear below  $\sim 1$  TeV, and thus be accessible at the LHC. For  $V_1^\pm$ , the sum rules (2) imply an inequality

$$g_{WZV}^{(1)} \lesssim \frac{g_{WWZ} M_Z^2}{\sqrt{3} M_1^\pm M_W}. \quad (5)$$

This bound is quite stringent ( $g_{WZV}^{(1)} \lesssim 0.04$  for  $M_1^\pm = 700$  GeV). Also, convergence of the sum rules (2) requires  $g_{WZV}^{(k)} \propto k^{-1/2} (M_k^\pm)^{-1}$ . The combination of heavier masses and lower couplings means that the heavier MVBs may well be unobservable, so that only the  $V_1$  states can be studied. The "saturation limit", in which there is only a single set of MVBs whose couplings saturate the sum rules, is likely to provide a good approximation to the phenomenology of the realistic Higgsless models. In this limit, the partial width of the  $V_1^\pm$  is given by

$$\Gamma(V_1^\pm \rightarrow W^\pm Z) \approx \frac{\alpha (M_1^\pm)^3}{144 \sin^2 \theta_W M_W^2}. \quad (6)$$

Given the couplings of the MVBs to the SM  $W$  and  $Z$ , we can now predict (at the parton level) the size of the new physics signals in the various channels of vector boson fusion. Fig. 3 provides an illustration for the case of  $WW \rightarrow WW$  and  $WZ \rightarrow WZ$ . We show the expected signal for either a SM Higgs boson of mass  $m_h = 500$  GeV, or the corresponding MVB  $V_1$  of mass 500 GeV in the saturation limit. The sum rules (4) govern the signal in the  $WW \rightarrow WW$  channel shown in the left panel of Fig. 3. However, the  $WW$  final state is difficult to observe over the SM backgrounds at the LHC: in the dilepton channel there is no resonance structure, while the jetty channels suffer from large QCD backgrounds. It is therefore rather challenging to test the sum rules (4). Notice that even if a  $WW$  resonance is observed, without a test of the sum rules (4), its interpretation is unclear, since the SM Higgs boson is *also* expected to appear as a  $WW$  resonance (see the left panel in Fig. 3).

We shall therefore concentrate on the  $WZ \rightarrow WZ$  channel, in which the Higgsless model predicts a series of resonances as in Fig. 1(e), while in the SM the amplitude is unitarized by the  $t$ -channel diagram of Fig. 1(d) and has no resonance (see the right panel in Fig. 3). Conventional theories of EWSB by strong dynamics may also contain a resonance in this channel, but it is likely to be heavy ( $\sim 2$  TeV for QCD-like theories) and broad due to strong coupling. In contrast, the MVB resonance is very narrow, as can be seen from Fig. 3 and Eq. (6). In fact it is almost a factor of 20 narrower than a SM Higgs boson of the same mass. This is primarily due to the vector nature of the MVB and our assumption that it only has a single decay channel. We therefore conclude that a resonance in the  $WZ \rightarrow WZ$  channel would be a smoking gun for the Higgsless model (for alternative interpretations involving extended Higgs sectors, see [15] and references therein). Finally, the  $WW \rightarrow ZZ$  channel is a good discriminator as well, since it will exhibit a resonance for the case of the SM but not the Higgsless models (see Fig. 2). A comparison of the resonant structure of the three vector boson fusion final states is shown in Table I.

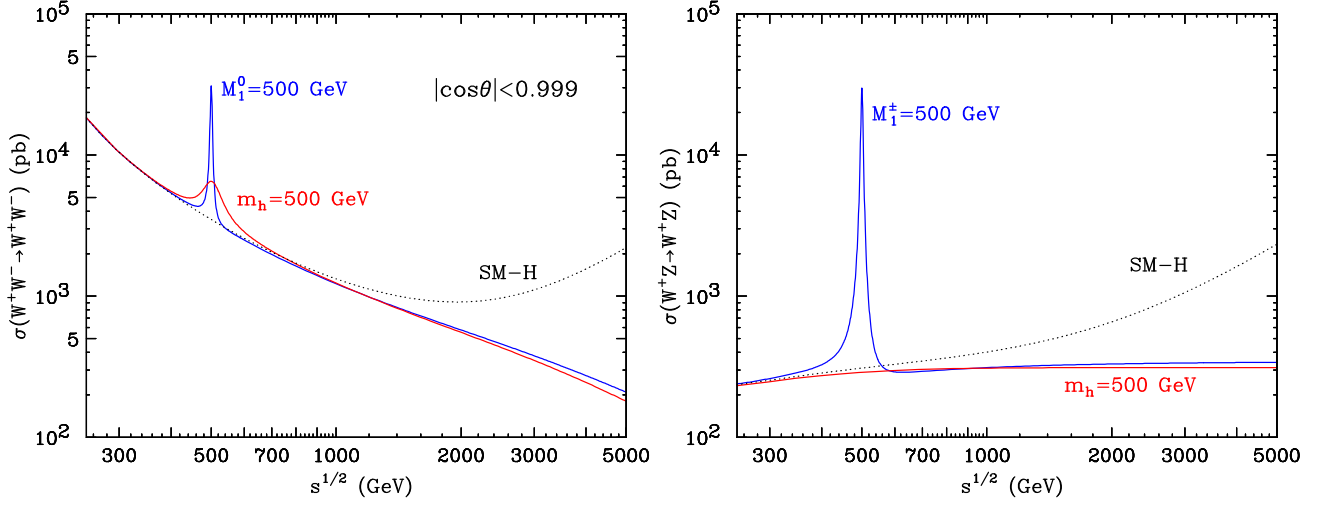


Figure 3: Elastic scattering cross-sections for  $WW \rightarrow WW$  (left) and  $WZ \rightarrow WZ$  (right) in the SM without a Higgs boson (SM-H) (dotted), the SM with a 500 GeV Higgs boson (red) and the Higgsless model with a 500 GeV MVB (blue).

Table I: Comparison of the resonance structure of the SM and Higgsless models in different vector boson fusion channels.

Model	$WW \rightarrow WW$	$WZ \rightarrow WZ$	$WW \rightarrow ZZ$
SM	Yes	No	Yes
Higgsless	Yes	Yes	No

### 3. COLLIDER PHENOMENOLOGY AT THE LHC

At the LHC, the vector boson fusion processes will occur as a result of  $W/Z$  bremsstrahlung off quarks. The typical final state for such events includes two forward jets in addition to a pair of gauge bosons. The production cross section of  $V_1^\pm$  in association with two jets is shown by the solid line in the left panel of Fig. 4. To estimate the prospects for the charged MVB search at the LHC, we require that both jets be observable (we assume jet rapidity coverage of  $|\eta| \leq 4.5$ ), and impose the following lower cuts on the jet rapidity, energy, and transverse momentum:  $|\eta| > 2$ ,  $E > 300$  GeV,  $p_T > 30$  GeV. These requirements enhance the contribution of the vector boson fusion diagrams relative to the irreducible background of the non-fusion  $q\bar{q}' \rightarrow WZ$  SM process as well as  $q\bar{q}' \rightarrow V_1^\pm$  Drell-Yan process. The “gold-plated” final state [17] for this search is  $2j + 3\ell + \cancel{E}_T$ , with the additional kinematic requirement that two of the leptons have to be consistent with a  $Z$  decay. We assume lepton rapidity coverage of  $|\eta| < 2.5$ . The  $WZ$  invariant mass,  $m_{WZ}$ , can be reconstructed using the missing transverse energy measurement and requiring that the neutrino and the odd lepton form a  $W$ . The number of “gold-plated” events (including all lepton sign combinations) in a  $300 \text{ fb}^{-1}$  LHC data sample, as a function of  $m_{WZ}$ , is shown in Fig. 4, for the SM (dotted), the Higgsless model with  $M_1^\pm = 700$  GeV (blue), and two “unitarization” models: Padé (red) and K-matrix (green) [16] (for details, see [13]). The Higgsless model can be easily identified by observing the MVB resonance: for the chosen parameters, the dataset contains  $130 V_1^\pm \rightarrow W^\pm Z \rightarrow 3\ell + \nu$  events. The irreducible non-fusion SM background is effectively suppressed by the cuts: the entire dataset shown in Fig. 4 contains only 6 such events. We therefore estimate the discovery reach for  $V_1^\pm$  resonance by requiring 10 signal events after cuts. The efficiency of the cuts for  $500 \text{ GeV} \leq M_1^\pm \leq 3 \text{ TeV}$  is in the range 20 – 25%. We then find that with  $10 \text{ fb}^{-1}$  of data, corresponding to 1 year of running at low luminosity, the LHC will probe the Higgsless models up to  $M_1^\pm \lesssim 550$  GeV, while covering the whole preferred range up to  $M_1^\pm = 1 \text{ TeV}$  requires  $60 \text{ fb}^{-1}$ . Note, however, that one should expect a certain amount of reducible background with fake and/or non-isolated leptons.

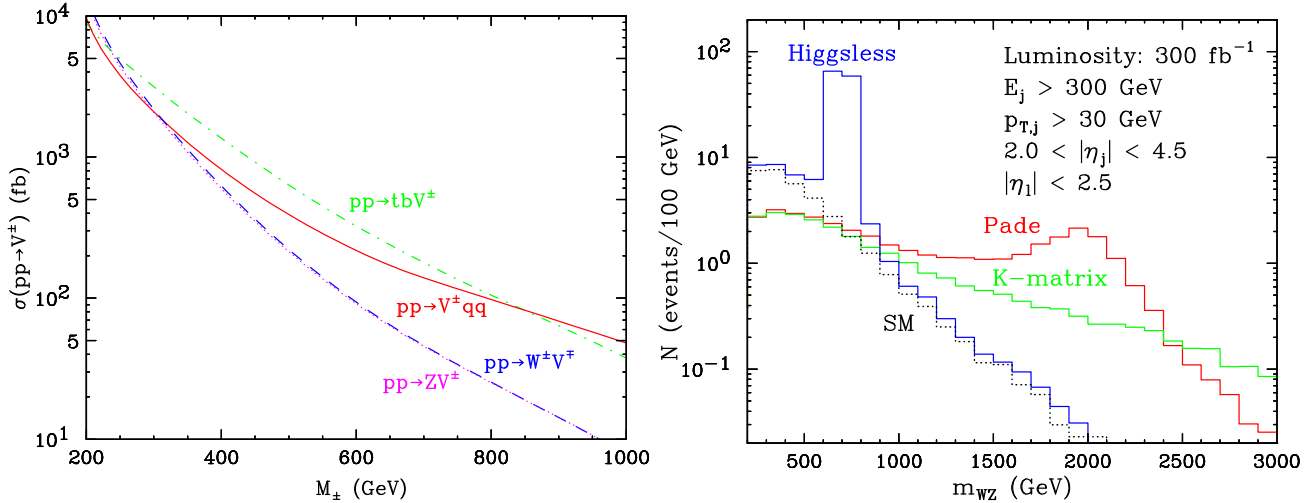


Figure 4: Left: Production cross-sections of  $V^\pm$  at the LHC. Here  $tbV^\pm$  production assumes SM-like couplings to third generation quarks. Right: The number of events per 100 GeV bin in the  $2j + 3\ell + \nu$  channel at the LHC with an integrated luminosity of  $300 \text{ fb}^{-1}$  and cuts as indicated in the figure. Results are shown for the SM (dotted), the Higgsless model with  $M_1^\pm = 700 \text{ GeV}$  (blue), and two "unitarization" models: Padé (red) and K-matrix (green) [16].

Once the  $V_1^\pm$  resonance is discovered, identifying it as part of a Higgsless model requires testing the sum rules (2) by measuring its mass  $M_1^\pm$  and coupling  $g_{WZV}^{(1)}$ . The coupling can be determined from the total  $V_1^\pm$  production cross section  $\sigma_{\text{tot}}$ . However, we are observing the  $V_1^\pm$  resonance in an exclusive channel, which only yields the product  $\sigma_{\text{tot}} BR(V_1^\pm \rightarrow W^\pm Z)$ . A measurement of the total resonance width  $\Gamma(V_1^\pm \rightarrow \text{anything})$  would remove the dependence on the unknown branching fraction  $BR$ . However, the accuracy of this measurement is severely limited by the poor missing energy resolution. Even though a Higgsless origin of the resonance can be ruled out if the value of  $g_{WZV}^{(1)}$ , inferred with the assumption of  $BR = 1$ , violates the bound (5), the LHC alone will not be able to settle the issue and precise measurements at the ILC appear to be necessary for the ultimate test of the theory.

## 4. COLLIDER PHENOMENOLOGY AT THE ILC

Unlike traditional technicolor, Higgsless models offer new discovery opportunities for a lepton collider with a center-of-mass energy in the sub-TeV range. From (3) we have seen that the masses of the new MVBs are expected to be below 1 TeV, and they can be produced at the ILC through the analogous vector boson fusion process by bremsstrahlung of  $W$ 's and  $Z$ 's off the initial state  $e^+$  and  $e^-$ . The  $V_1$  production cross-sections for vector boson fusion  $e^+e^- \rightarrow V_1^\pm e^\mp \nu_e$  and  $e^+e^- \rightarrow V_1^0 \nu_e \bar{\nu}_e$  as well as associated production  $e^+e^- \rightarrow V^\pm W^\mp$  are shown in the left panel of Fig. 5. The horizontal lines correspond to the total cross-section of the continuum SM background. We see that for a large range of  $V_1$  masses, ILC searches appear promising, already at the level of total number of events, before cuts and efficiencies. Furthermore, because of the cleaner environment of the ILC, one can now use the dominant hadronic decay modes of the  $W$  and  $Z$ , and easily reconstruct the invariant mass of the  $V_1$  resonance, which provides an extra handle for background suppression (see the right panel in Fig. 5). Further detailed studies are needed to better evaluate the ILC potential for testing the generic predictions (2) and (4) of the Higgsless models.

## Acknowledgments

MP is supported by NSF grant PHY-0355005. KM and AB are supported by a US DoE Outstanding Junior Investigator award under grant DE-FG02-97ER41029.

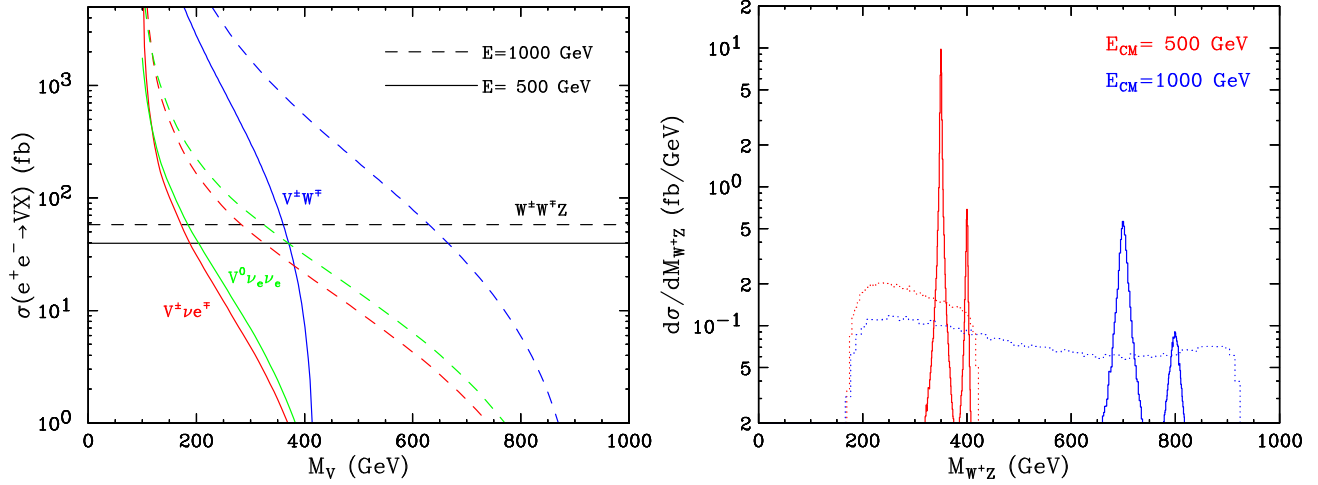


Figure 5: Left:  $V_1$  production cross-sections and the continuum SM background at an  $e^+e^-$  lepton collider of center of mass energy 500 GeV (solid) or 1 TeV (dashed). Right:  $WZ$  invariant mass distribution for Higgsless signals (solid) and SM background (dotted), at  $E_{CM} = 500$  GeV (red,  $M^\pm = 350, 400$  GeV) and  $E_{CM} = 1$  TeV (blue,  $M^\pm = 700, 800$  GeV).

## References

- [1] S. Dimopoulos and L. Susskind, Nucl. Phys. B **155**, 237 (1979); L. Susskind, Phys. Rev. D **20**, 2619 (1979); S. Weinberg, Phys. Rev. D **19**, 1277 (1979).
- [2] M. E. Peskin and T. Takeuchi, Phys. Rev. Lett. **65**, 964 (1990); Phys. Rev. D **46**, 381 (1992).
- [3] C. Csaki *et al.*, Phys. Rev. D **69**, 055006 (2004) [arXiv:hep-ph/0305237].
- [4] C. Csaki, C. Grojean, L. Pilo and J. Terning, Phys. Rev. Lett. **92**, 101802 (2004) [arXiv:hep-ph/0308038].
- [5] Y. Nomura, JHEP **0311**, 050 (2003) [arXiv:hep-ph/0309189].
- [6] C. Csaki *et al.*, Phys. Rev. D **70**, 015012 (2004) [arXiv:hep-ph/0310355].
- [7] G. Cacciapaglia, C. Csaki, C. Grojean and J. Terning, Phys. Rev. D **71**, 035015 (2005) [arXiv:hep-ph/0409126]; R. Foadi, S. Gopalakrishna and C. Schmidt, Phys. Lett. B **606**, 157 (2005) [arXiv:hep-ph/0409266]; C. Schwinn, Phys. Rev. D **71**, 113005 (2005) [arXiv:hep-ph/0504240]; G. Cacciapaglia *et al.*, arXiv:hep-ph/0505001.
- [8] R. Sekhar Chivukula, D. A. Dicus and H. J. He, Phys. Lett. B **525**, 175 (2002) [arXiv:hep-ph/0111016].
- [9] R. Barbieri, A. Pomarol and R. Rattazzi, Phys. Lett. B **591**, 141 (2004) [arXiv:hep-ph/0310285]; G. Burdman and Y. Nomura, Phys. Rev. D **69**, 115013 (2004) [arXiv:hep-ph/0312247]; G. Cacciapaglia, C. Csaki, C. Grojean and J. Terning, Phys. Rev. D **70**, 075014 (2004) [arXiv:hep-ph/0401160].
- [10] H. Davoudiasl, J. L. Hewett, B. Lillie and T. G. Rizzo, Phys. Rev. D **70**, 015006 (2004) [arXiv:hep-ph/0312193].
- [11] H. Davoudiasl, J. L. Hewett, B. Lillie and T. G. Rizzo, JHEP **0405**, 015 (2004) [arXiv:hep-ph/0403300]; R. Barbieri, A. Pomarol, R. Rattazzi and A. Strumia, Nucl. Phys. B **703**, 127 (2004) [arXiv:hep-ph/0405040]; J. L. Hewett, B. Lillie and T. G. Rizzo, JHEP **0410**, 014 (2004) [arXiv:hep-ph/0407059].
- [12] R. Foadi, S. Gopalakrishna and C. Schmidt, JHEP **0403**, 042 (2004) [arXiv:hep-ph/0312324]; R. Casalbuoni, S. De Curtis and D. Dominici, Phys. Rev. D **70**, 055010 (2004) [arXiv:hep-ph/0405188]; R. S. Chivukula *et al.*, Phys. Rev. D **70**, 075008 (2004) [arXiv:hep-ph/0406077]; H. Georgi, Phys. Rev. D **71**, 015016 (2005) [arXiv:hep-ph/0408067]; M. Perelstein, JHEP **0410**, 010 (2004) [arXiv:hep-ph/0408072]; H. Georgi, arXiv:hep-ph/0508014.
- [13] A. Birkedal, K. Matchev and M. Perelstein, Phys. Rev. Lett. **94**, 191803 (2005) [arXiv:hep-ph/0412278].
- [14] M. Papucci, arXiv:hep-ph/0408058.
- [15] E. Asakawa and S. Kanemura, arXiv:hep-ph/0506310.
- [16] A. Dobado, M. J. Herrero and J. Terron, Z. Phys. C **50** (1991) 205; Z. Phys. C **50** (1991) 465.
- [17] J. Bagger *et al.*, Phys. Rev. D **49**, 1246 (1994) [arXiv:hep-ph/9306256]; Phys. Rev. D **52**, 3878 (1995) [arXiv:hep-ph/9504426]. See also M. S. Chanowitz, arXiv:hep-ph/0412203 and references therein.